Anlotinib suppresses proliferation, migration, and immune escape of gastric cancer cells by activating the cGAS-STING/IFN-β pathway

Min YUAN[1], Xian-Ling GUO[1], Jian-Hua CHEN[1], Yang HE[1,2], Zhu-Qing LIU[1], He-Ping ZHANG[1], Jie REN[1], Qing XU[1,*]

[1]Department of Oncology, Shanghai Tenth People's Hospital, Tongji University, Shanghai, China; [2]Department of Interventional Oncology, Shanghai DaHua Hospital, Shanghai, China

*Correspondence: 2713600@163.com

This article reported the mechanism of Anlotinib in gastric cancer treatment. Gastric cancer cells were treated with Anlotinib (8 μM) and transfected by STING shRNA and STING vectors. Cell counting kit-8 assay, wounding healing assay, and Transwell experiment were applied for proliferation, migration, and invasion detection. PD-L1 fluorescence intensity in gastric cancer cells was explored by flow cytometry. IFN-β level was researched by enzyme-linked immunosorbent reaction. Xenograft tumor experiment was performed by administering mice with Anlotinib and anti-PD-L1 antibody. Immuno-histochemistry and western blot were used for proteins expression detection. Quantitative real-time reverse transcription-polymerase chain reaction was applied for mRNA expression detection. Hematoxylin and eosin staining was conducted on lung, liver, kidney, and cerebral cortex of mice. Gastric cancer cells treated with Anlotinib exhibited reduced proliferation, migration, and invasion (p<0.01). Anlotinib treatment reduced PCNA, CDK1, and MMP2 protein expressions and increased E-cadherin protein expression in gastric cancer cells (p<0.01). Anlotinib treatment suppressed PD-L1 expression and activated the cGAS-STING/IFN-β pathway in gastric cancer cells (p<0.01). STING knockdown partially reversed the inhibition of Anlotinib on gastric cancer cells proliferation, migration, invasion, and immune escape (p<0.05 or p<0.01). However, STING overexpression exhibited the opposite effect. Anlotinib synergistically improved anti-tumor efficacy of anti-PD-L1 in vivo. Anlotinib synergistic anti-PD-L1 increased CD3+, CD8+ T cells, and activated the cGAS-STING/IFN-β pathway in xenograft tumor. Anlotinib was non-toxic to lung, liver, cortex, and kidney. Anlotinib suppressed gastric cancer cells proliferation, migration, and immune escape by activating the cGAS-STING/IFN-β pathway.

Key words: gastric cancer, Anlotinib, cGAS-STING/IFN-β pathway, proliferation, immune escape

Gastric cancer is the most common gastrointestinal cancer and is the third leading cause of cancer-related deaths in the world [1]. The tumorigenesis of gastric cancer involves multiple factors, such as *Helicobacter pylori* infection, excessive salt intake, gastric ulcers, alcoholism, and genetic factors [2]. According to the statistics, about 8.2% of cancer-related deaths were due to gastric cancer [3]. The 5-year overall survival of gastric cancer cases is still less than 30% despite great advancements in diagnosis and treatment [4]. A large proportion of gastric cancer patients develop advanced tumors at initial diagnosis, thereby leading to a worse prognosis [5]. The standard treatment for gastric cancer is surgical resection and postoperative chemotherapy [6]. Several chemotherapeutic drugs for gastric cancer have appeared clinically. However, the unsatisfactory chemotherapy effect is one of the main reasons for gastric cancer recurrence and metastasis postoperative [7]. Therefore, it is of great importance to find more effective drugs for gastric cancer chemotherapy.

Anlotinib is a multitarget tyrosine kinase inhibitor, which possesses antitumor effects in multiple solid tumors. Clinical trials had been discovered that Anlotinib was conducive to hepatocellular carcinoma, renal carcinoma, non-small cell lung cancer treatment [8, 9]. In a recurrent glioblastoma case, Anlotinib showed a well therapeutic effect. The case exhibited partial response after 2 months of treatment with Anlotinib [10]. Phase III trial about refractory metastatic colorectal cancer cases indicated that Anlotinib administration obviously improved patients' progression-free survival, objective remission rate, and disease control rate [11]. For advanced non-small cell lung cancer, Anlotinib showed well tolerability and effectiveness [12]. Additionally, Anlotinib improved the overall survival and progression-free survival of refractory epithelial ovarian cancer cases [13]. All of this

evidence illustrated that Anlotinib might be a novel and effective treatment option for cancer patients. Recently, studies revealed that Anlotinib might be useful for the treatment of gastric cancer [14, 15]. However, currently available data about Anlotinib in gastric cancer treatment are still limited.

Tumor immune escape is an important way for tumors to survive and metastasize, and immunosuppression is one of the main mechanisms for tumor immune escape. Immunosuppression can suppress T lymphocytes' activation and enhance tumor cells' immune tolerance, resulting in tumor cells' immune escape [16]. Programmed death ligand-1 (PD-L1) is an essential member of tumor immunosuppression, which helps tumor cells escape from immune surveillance [17]. Therefore, this study researched the effect of Anlotinib on gastric cancer progression by exploring its effect on immune escape. It was hoped that the findings in this paper could provide a more theoretical basis for the clinical application of Anlotinib in gastric cancer treatment.

Materials and methods

Gastric cell lines and culture. Gastric cell lines, AGS and HS746T, were purchased from the American Type Culture Collection (ATCC, Manassas, VA, USA). Dulbecco's modified Eagle's medium (DMEM, Solarbio, Beijing, China) containing 10% fetal bovine serum (FBS, Solarbio, Beijing, China) was applied to culture cells at 37 °C and 5% CO_2 in a humidified incubator.

Anlotinib treatment. DMEM containing 10% FBS and Anlotinib (a final concentration of 0.25, 0.5, 1, 2, 4, 8, 16, and 32 μM) was prepared. AGS and HS746T cells were collected in the logarithmic growth period, followed by being cultured with DMEM containing 10% FBS and Anlotinib at 37 °C and 5% CO_2. AGS and HS746T cells cultured in DMEM containing 10% FBS were used as the control group, and those cultured in DMEM containing 10% FBS and 8 μM Anlotinib served as the Anlotinib group.

Cell transfection and Anlotinib treatment. AGS cells were harvested in the logarithmic growth period. Phosphate buffered saline (PBS) was applied to wash AGS cells 3 times. Then AGS cells were prepared into cell suspension by using DMEM (without FBS) with a density of 1×10^6 cells/ml. The AGS cell suspension was plated into 6-well plates with 1 ml/well. STING shRNA and negative control, STING expression vectors and empty vectors were all purchased from GeneChem (Shanghai, China). According to the instruction of Lipofectamine 3000 (Thermo Fisher Scientific, Waltham, MA, USA), AGS cells were transfected by STING shRNA, negative control, STING expression vectors, and empty vectors. Post-transfection, AGS cells transfected by negative control and empty vectors were cultured in DMEM containing 10% FBS (Control+shNC group and Control+NC group), or with DMEM containing 10% FBS and Anlotinib (a final concentration of 8 μM) (Anlotinib+shNC group and Anlotinib+NC group). AGS cells transfected by STING

shRNA and STING expression vectors were cultured in DMEM containing 10% FBS and Anlotinib (a final concentration of 8 μM) (Anlotinib+shSTING group and Anlotinib+STING group). AGS cells of the three groups were kept at 37 °C and 5% CO_2.

Cell counting kit-8 (CCK-8) assay. Cell proliferation was reflected by the CCK-8 assay. Using 96-well plates, AGS and HS746T cells (1×10^4 cells) were cultured in 100 μl of DMEM containing 10% FBS and different concentrations of Anlotinib (a final concentration of 0.25, 0.5, 1, 2, 4, 8, 16, and 32 μM) at 37 °C and 5% CO_2 for 48 h. Additionally, AGS cells (1×10^4 cells) of Control+shNC group, Anlotinib+shNC group, and Anlotinib+shSTING group were cultured in 96-well plates with 100 μl of a medium at 37 °C and 5% CO_2 for 48 h. After that, CCK-8 solution was added to treat cells for 2 h at 37 °C. The optical density (OD) value was measured using a multi-well microplate reader.

Wounding healing assay. AGS and HS746T cells of Control group and Anlotinib group, as well as AGS cells of Control+shNC group, Anlotinib+shNC group, and Anlotinib+shSTING group, were grown in 6-well plates (1×10^7 cells/well) using 1 ml of a medium at 37 °C and 5% CO_2. After culturing for 24 h, a wound was made using a sterile pipette tip through the center of each well bottom. The wound width was labeled as the initial wound width. Cells were cultured with fresh medium for another 24 h at 37 °C and 5% CO_2. The wound width was measured and labeled as the final wound width. Relative wound width was calculated by final wound width/initial wound width.

Transwell experiment. Matrigel (Boster, Wuhan, China) was used to pre-coat the 6-well Transwell inserts (8 μm pore size). AGS and HS746T cells of Control group and Anlotinib group, and AGS cells of Control+shNC group, Anlotinib+shNC group, and Anlotinib+shSTING group, were plated into the upper chambers of 6-well inserts (1×10^4 cells per insert) using 500 μl of a medium (without FBS). A total of 600 μl DMEM containing 10% FBS was plated into the lower chambers. Cells were maintained for 48 h at 37 °C and 5% CO_2. The invasion cells were fixed with 4% paraformaldehyde and stained with 0.1% violet crystal, followed by being counted under a microscope. The number of invasion cells was counted in 5 random fields of view.

Flow cytometry. AGS and HS746T cells (1×10^6 cells) of Control group and Anlotinib group, and AGS cells of Control+shNC group, Anlotinib+shNC group, and Anlotinib+shSTING group (1×10^6 cells), were treated by pre-cooled 70% alcohol for 1 h at 4 °C. PBS was applied to wash cells 3 times. Goat serum was added into cells to block cells for 1 h at room temperature. Cells were probed by anti-human PD-L1 antibody (1:100, ab205921, Abcam, Cambridge, UK) or control IgG (1:100, ab17273, Abcam, Cambridge, UK) for 12 h at 4 °C. After washing with PBS, cells were treated for 2 h by using Alexa Fluor 488 conjugated anti-rabbit IgG second antibody (1:2000, ab150077, Abcam, Cambridge, UK) at room temperature. PD-L1 fluorescence

intensity of cells in each group was detected by a FACSCalibur flow cytometer (Becton Dickinson, Franklin Lakes, NJ, USA).

Enzyme-linked immunosorbent reaction (ELISA). AGS and HS746T cells ($1×10^5$ cells) of Control group and Anlotinib group, and AGS cells ($1×10^5$ cells) of Control+shNC group, Anlotinib+shNC group, and Anlotinib+shSTING group, were grown in 6-well plates with 1 ml medium for 48 h at 37°C and 5% CO_2. Afterward, cells were harvested and washed 3 times using PBS. According to the instruction of the ELISA kit (Kanglang Biological Technology, Shanghai, China), the level of IFN-β in gastric cancer cells was detected.

In vivo **study.** A total of 20 C57BL/6 mice (6 weeks old) were purchased from the Shanghai Animal Experiment Center, Chinese Academy of Sciences. All mice were kept in a 22°C room under pathogen-free conditions. Water and food were freely available for all mice. This study has been approved by the animal ethics committee of Shanghai Tenth People's Hospital. The animal experiment was conducted in line with the Guide for the Care and Use of Laboratory Animals.

Mice of randomly divided into 4 groups: NC group (n=5), Anlotinib group (n=5), Anti-PD-L1 group (n=5), and Anlotinib+Anti-PD-L1 group (n=5). A total of $1×10^6$ AGS cells (dispersed into 100 μl PBS) were injected subcutaneously into the back of all mice. After 7 days of cells inoculation, mice of Anlotinib group and Anlotinib+Anti-PD-L1 group were administered through oral gavage for 2 consecutive weeks. The dose of Anlotinib was 1.5 mg/kg every day. For mice of Anti-PD-L1 group and Anlotinib+Anti-PD-L1 group, anti-PD-L1 antibody (200 μg/mouse/5 days) was injected subcutaneously after 11 days of cells inoculation. The injection frequency of the anti-PD-L1 antibody was every 5 days [18]. From cells inoculation, the tumor volume was measured every 7 days using (length×width^2)/2. On the 28th day of inoculation, mice were euthanized after being anesthetized by subcutaneous injection of pentobarbital (60 mg/kg). The xenograft tumor of each group was removed. After being weighted, the xenograft tumor was stored at −80°C immediately. Simultaneously, lung, liver, kidney, and cerebral cortex of mice in each group were obtained and stored at −80°C immediately.

Immunohistochemistry (IHC). Xenograft tumor tissues were fixed with 10% formaldehyde solution for 24 h at 4°C. Tissues were cut into sections after embedding into paraffin. Sections were baked at 60°C for 20 min, followed by being treated with xylene for 10 min. Gradient alcohol was used to immerse sections for rehydration. After antigen retrieval, sections were treated with 0.1% Triton X-100 for 5 min and 3% H_2O_2 for 30 min. Goat serum was added to treat sections for 30 min at room temperature. Primary antibodies (1:200) were added to treat sections overnight at 4°C. Primary antibodies were as below: rabbit anti-cGAS (ab224144, Abcam, Shanghai, China), rabbit anti-STING (ab252560, Abcam, Shanghai, China), rabbit anti-CD3 (ab16669,

Abcam, Shanghai, China), rabbit anti-CD8 (ab217344, Abcam, Shanghai, China), and rabbit anti-IFN-β (XY-500-P32B-50, Xiyuan Biological Technology, Shanghai, China). Then, goat anti-rabbit secondary antibody (1:200, ab205718, Abcam, Shanghai, China) was used to treat sections for 2 h at room temperature. The color reaction was achieved by dripping (DAB) onto the sections. Hematoxylin was used for counterstaining the sections. Sections were sealed in neutral resin before being observed under a microscope.

Western blot. Gastric cancer cells of each group were collected and lysed by RIPA buffer for 30 min on ice. The lysate was centrifuged at 12,000×g for 15 min at 4°C. The supernatant containing total proteins was harvested. The BCA kit was responsible for total protein concentration detection based on the manual. After that, 30 μg total proteins underwent separation at 40 V for 4 h through sodium dodecyl sulfate-polyacrylamide gel electrophoresis (SDS-PAGE). At 60 V, total proteins were electrotransferred onto polyvinylidene fluoride (PVDF) membrane for 2 h. The membrane was immersed in 5% non-fat milk for 2 h blocking. After being probed by primary antibodies (1:1000) for 12 h at 4°C, the PVDF membrane was incubated with horseradish peroxidase (HRP)-conjugated goat anti-rabbit secondary antibody (1:2000, ab6721, Abcam, Shanghai, China) for 2 h at room temperature. Primary antibodies were as below: rabbit anti-PCNA (1:1000, ab18197, Abcam, Shanghai, China), rabbit anti-CDK1 (1:1000, ab131450, Abcam, Shanghai, China), rabbit anti-MMP2 (1:1000, ab97779, Abcam, Shanghai, China), rabbit anti-E-cadherin (1:1000, ab15148, Abcam, Shanghai, China), rabbit anti-PD-L1 (1:1000, ab233482, Abcam, Shanghai, China), rabbit anti-cGAS (1:1000, ab224144, Abcam, Shanghai, China), rabbit anti-STING (1:1000, ab252560, Abcam, Shanghai, China), rabbit anti-IFN-β (1:1000, XY-500-P32B-50, Xiyuan Biological Technology, Shanghai, China), and rabbit anti-GAPDH (1:1000, ab9485, Abcam, Shanghai, China). An enhanced chemiluminescence reagent (Boster, Wuhan, China) was added to the PVDF membrane to develop protein bands. The proteins were quantified using ImageJ software with GAPDH as a control.

Quantitative real-time reverse transcription-polymerase chain reaction (qRT-PCR). Gastric cancer cells were collected and washed 3 times by PBS. Total RNA in cells was extracted using Trizol reagent according to the manual. Additionally, total RNA in xenograft tumor tissues was also extracted using the same method. Prime Script TM RT reagent Kit (Takara, Dalian, China) was applied for the synthesis of cDNA in line with the manual. An ABI 7900 system (Applied BioSystems, Foster City, CA, USA) was responsible for PCR analysis. The parameters were as below: 10 min at 95°C, and 39 cycles of 15 s at 95°C and 60 s at 60°C. mRNAs relative expression was determined by the $2^{-\Delta\Delta Ct}$ method. The primers were: cGAS, sense 5'-ATGCAAAGGAAGGAAATGGT-3' and anti-sense 5'-TTTAAACAATCTTTCCTGCAACA-3'. STING, sense 5'-GAGCAGGCCAAACTCTTCTG-3'

and anti-sense 5'-TGCCCACAGTAACCTCTTCC-3'. IFN-β, sense 5'-GTCTCCTCCAAATTGCTCTC-3' and anti-sense 5'-ACAGGAGCTTCTGACACTGA-3'. Granzyme B, sense 5'-CCTGGGAAAACACTCACAC-3' and anti-sense 5'-CACGCACAACTCAATGGTA-3'. TNF-α, sense 5'-GGAAAGGACACCATGAGC-3', anti-sense 5'-CCACGATCAGGAAGGAGA-3'. IFN-g, sense 5'-TGGGTTCTCTTGGCTGTTA-3', anti-sense 5'-TTCTGTCACTCTCCTCTTTCC-3'. CCL5 sense 5'-GCAGAGGATCAAGACAGCA-3', anti-sense 5'-GGG-CAGTAGCAATGAGGA-3'. CXCL9, sense 5'-GGGACTATC-CACCTACAATCC-3', anti-sense 5'-AATCAGTTCCTTCA-CATCTGC-3'. CXCL10, sense 5'-AAGCAGTTAGCAAGGAA-AGG-3', anti-sense 5'-GTAGGGAAGTGATGGGAGAG-3'. IL1b, sense 5'-TTGAGTCTGCCCAGTTCC-3', anti-sense 5'-TTTCTGCTTGAGAGGTGCT-3'. IL12b, sense 5'-GGT-ATCACCTGGACCTTG-3', anti-sense 5'-GCGAATGGC-TTAGAACCTC-3'. IL15, sense 5'-CATTTTGGGCTGTT-TCAGT-3', anti-sense 5'-TTACATTCACCCAGTTGGC3'. IL17a, sense 5'-CTGATGGGAACGTGGACT-3', anti-sense 5'-ACTGCTTTGGGGAGTGTG-3'. GAPDH, sense 5'-CAGAACATCATCCCTGCCTCT-3' and anti-sense 5'-GCTTGACAAAGTGGTCGTTGAG-3'. GAPDH was used as an internal control.

Hematoxylin and eosin (HE) staining. Lung, liver, kidney, and cerebral cortex of mice in each group were fixed with 10% formaldehyde solution for 24 h at 4 °C. These tissues were then embedded in paraffin, followed by being cut into tissue sections. After being treated with xylene, tissue sections were rehydrated by gradient alcohol. Thereafter, hematoxylin and eosin were sequentially used to stain tissue sections for 3 min. Dehydration of tissue sections was achieved by gradient alcohol. Tissue sections were transparentized before being sealed in neutral resin. The structure and damage of tissue sections were observed under a microscope.

Statistical analysis. All data were exhibited as mean ± standard deviation and processed by SPSS 19.0 software. Student's t-test was for the difference analysis between the two groups. One-way analysis of variance (ANOVA) with Tukey's post hoc test was for the difference analysis in multiple groups (more than two groups). A p-value <0.05 indicated a statistically significant difference.

Results

Anlotinib inhibited the proliferation and invasion of gastric cancer cells. Anlotinib at different doses was used to treat gastric cancer cells. Gastric cancer cells treated by 2, 4, 8, 16, and 32 μM Anlotinib showed lower cell proliferation ability than gastric cancer cells without any treatment (p<0.05, p<0.01, or p<0.001). Anlotinib at doses of 0.25, 0.5, and 1 μM did not affect cell proliferation ability when compared with gastric cancer cells without any treatment (Figure 1A). In a subsequent study, Anlotinib at a dose of 8 μM was selected to treat gastric cancer cells (set as the

Anlotinib group). Gastric cancer cells without any treatment were set as the Control group.

The wound-healing assay revealed higher relative wound width in gastric cancer cells of the Anlotinib group compared with the Control group (p<0.01, Figure 1B). By Transwell experiment, gastric cancer cells of the Anlotinib group exhibited a decreased invasion ability than the Control group (p<0.01, Figure 1C). Relative to the Control group, reduced PCNA, CDK1, MMP2 protein expression, and enhanced E-cadherin protein expression were seen in gastric cancer cells of the Anlotinib group (p<0.01, Figure 1D).

Anlotinib suppressed the PD-L1 expression but activated the cGAS-STING/IFN-β pathway in gastric cancer cells. This study used western blot to detect PD-L1 expression in gastric cancer cells. Compared with the Control group, gastric cancer cells of the Anlotinib group expressed lower PD-L1 protein levels (p<0.01, Figure 2A). Consistently, flow cytometry revealed lower PD-L1 fluorescence intensity in gastric cancer cells of the Anlotinib group when compared with the Control group (p<0.01, Figure 2B). The mRNAs and protein expressions of cGAS, STING, and IFN-β in gastric cancer cells were explored by qRT-PCR and western blot. As a result, higher mRNA and protein expressions of cGAS, STING, and IFN-β occurred in gastric cancer cells of the Anlotinib group when compared with the Control group (p<0.01, Figures 2C–D). ELISA was utilized to detect the level of IFN-β in gastric cancer cells. In comparison with the Control group, a higher IFN-β level in gastric cancer cells of the Anlotinib group was observed (p<0.01, Figure 2E).

Anlotinib inhibited gastric cancer cell proliferation, migration, and immune escape by activating the cGAS-STING/IFN-β pathway. Gastric cancer cells of the Anlotinib+shNC group displayed lower cell proliferation ability, higher relative wound width, and lower invasion ability than that of the Control+shNC group (all p<0.01). Compared with the Anlotinib+shNC group, gastric cancer cells of the Anlotinib+shSTING group presented higher cell proliferation ability, lower relative wound width, and higher invasion ability (p<0.05 or p<0.01, Figures 3A–C). In comparison with the Control+shNC group, gastric cancer cells of the Anlotinib+shNC group expressed lower PCNA, CDK1, MMP2 proteins, and higher E-cadherin protein levels (p<0.01). However, higher PCNA, CDK1, MMP2 protein expressions, and lower E-cadherin protein expression occurred in gastric cancer cells of the Anlotinib+shSTING group when relative to the Anlotinib+shNC group (p<0.01, Figure 3D). Western blot and flow cytometry demonstrated lower PD-L1 protein level and fluorescence intensity in gastric cancer cells of the Anlotinib+shNC group when compared with the Control+shNC group (p<0.01). Oppositely, compared with the Anlotinib+shNC group, PD-L1 protein level and fluorescence intensity were increased in gastric cancer cells of the Anlotinib+shSTING group (p<0.01, Figures 3E–F). ELISA revealed an increased IFN-β protein level in gastric cancer cells of the Anlotinib+shNC
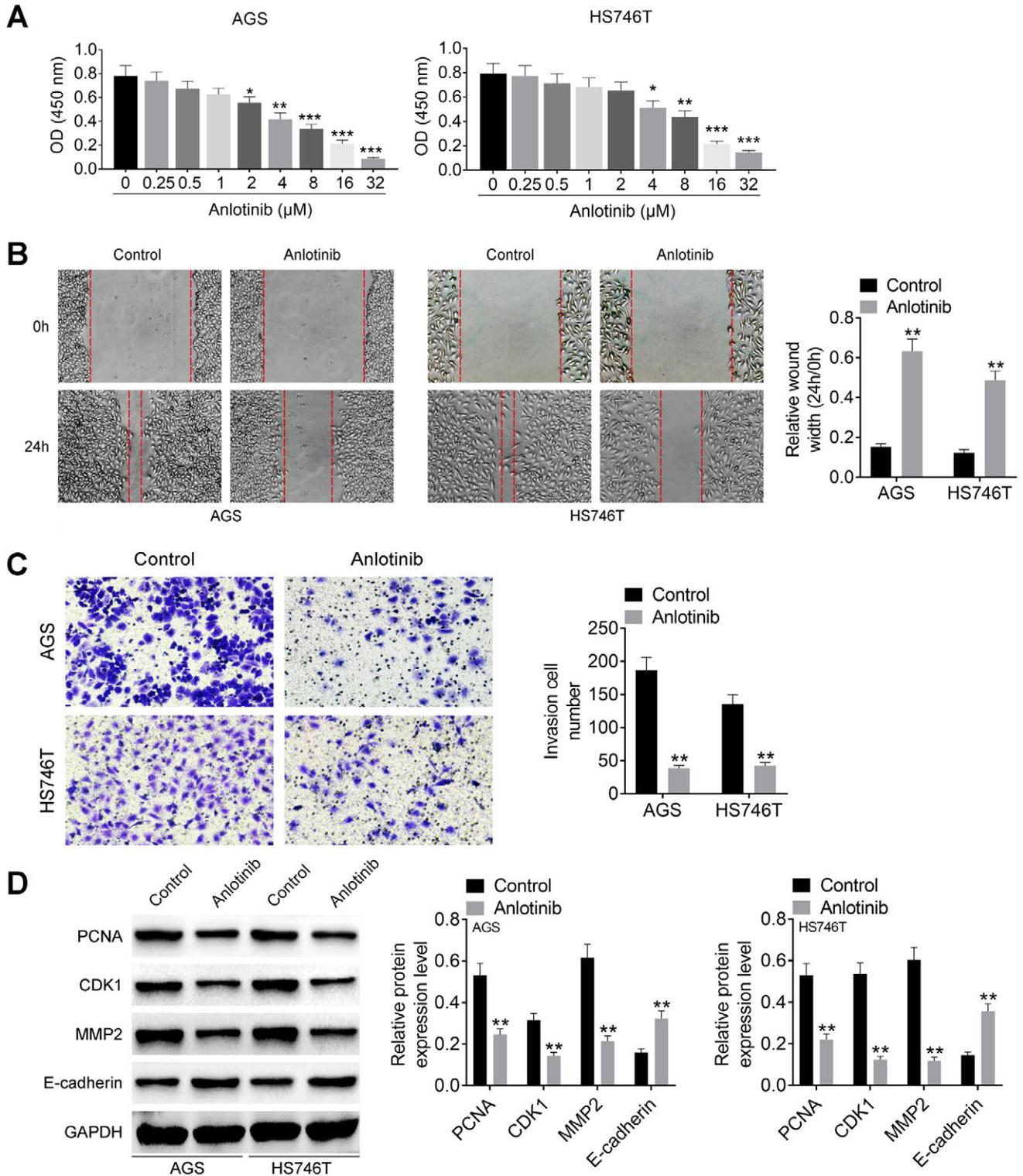
Figure 1. Anlotinib inhibited the proliferation and invasion of gastric cancer cells. A) Proliferation of gastric cancer cells by CCK-8 assay. *p<0.05, **p<0.01, and ***p<0.001 vs. gastric cancer cells without any treatment. B) Migration of gastric cancer cells by wound-healing experiment. **p<0.01 vs. the Control group. C) Invasion of gastric cancer cells by Transwell experiment. **p<0.01 vs. the Control group. D) Proteins expression in gastric cancer cells by western blot. **p<0.01 vs. the Control group
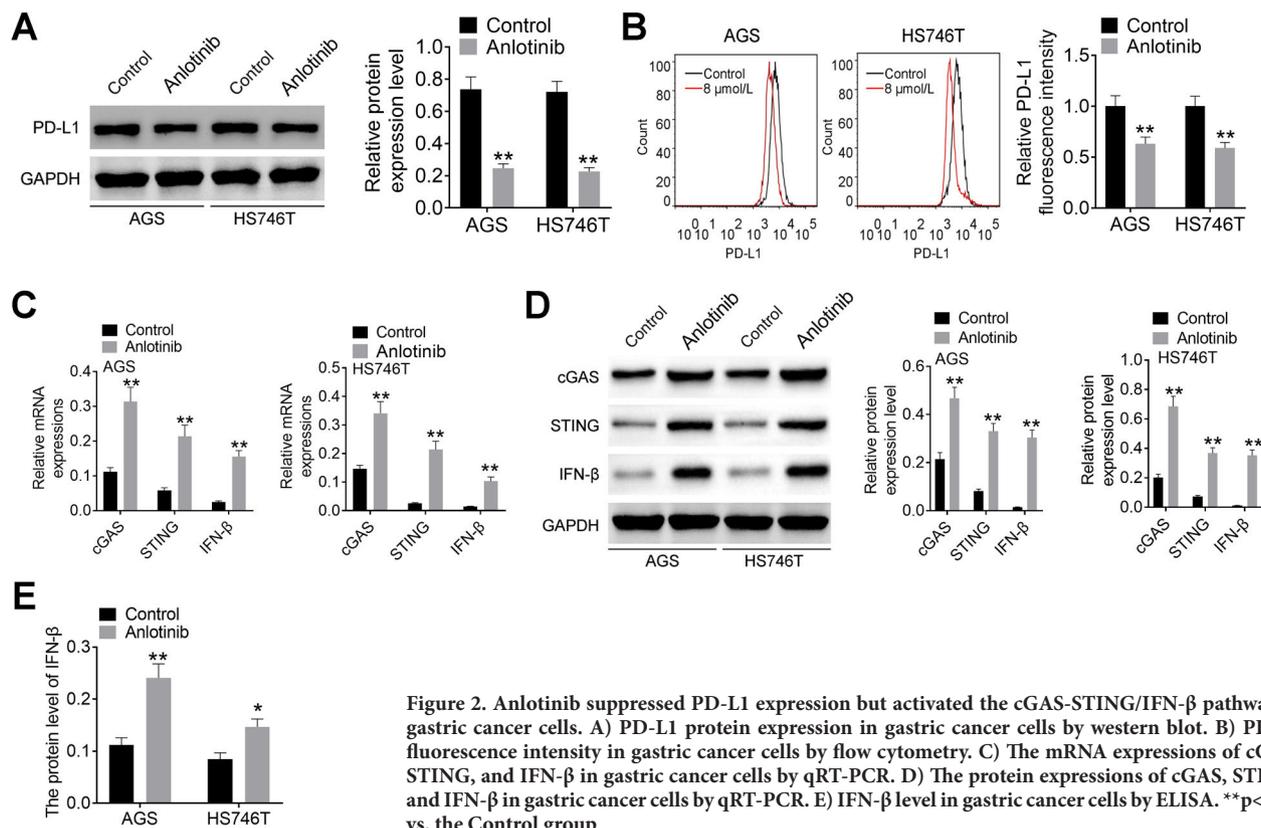
Figure 2. Anlotinib suppressed PD-L1 expression but activated the cGAS-STING/IFN-β pathway in gastric cancer cells. A) PD-L1 protein expression in gastric cancer cells by western blot. B) PD-L1 fluorescence intensity in gastric cancer cells by flow cytometry. C) The mRNA expressions of cGAS, STING, and IFN-β in gastric cancer cells by qRT-PCR. D) The protein expressions of cGAS, STING, and IFN-β in gastric cancer cells by qRT-PCR. E) IFN-β level in gastric cancer cells by ELISA. **p<0.01 vs. the Control group

group relative to the Control+shNC group (p<0.01). A reduced IFN-β level was observed in gastric cancer cells of the Anlotinib+shSTING group when compared with the Anlotinib+shNC group (p<0.05, Figure 3G).

Additionally, in comparison to the Control+NC group, lower cell proliferation ability, higher relative wound width, and lower invasion ability were observed in gastric cancer cells of the Anlotinib+NC group (p<0.01). Relative to the Anlotinib+NC group, gastric cancer cells of the Anlotinib+STING group had lower cell proliferation ability, higher relative wound width, and lower invasion ability (p<0.01, Figures 4A–C). Western blot exhibited that gastric cancer cells of the Anlotinib+NC group expressed lower PCNA, CDK1, MMP2 protein levels, and higher E-cadherin protein level than the Control+NC group (p<0.01). Lower PCNA, CDK1, MMP2 protein expressions, and higher E-cadherin protein expression occurred in gastric cancer cells of the Anlotinib+STING group when relative to the Anlotinib+NC group (p<0.01, Figure 4D). Meanwhile, lower PD-L1 protein level and fluorescence intensity in gastric cancer cells of the Anlotinib+NC group were found when compared to the Control+NC group (p<0.01). Gastric cancer cells of the Anlotinib+STING group also displayed lower PD-L1 protein level and fluorescence intensity than that of the Anlotinib+NC group (p<0.01, Figures 4E–F). A higher IFN-β level was presented in gastric cancer cells of

the Anlotinib+NC group in comparison to the Control+NC group (p<0.01). At the same time, the IFN-β level was higher in gastric cancer cells of the Anlotinib+STING group when relative to the Anlotinib+NC group (p<0.05, Figure 4G). All of the above data indicated that Anlotinib might inhibit gastric cancer cell proliferation, migration, and immune escape by activating the cGAS-STING/IFN-β pathway.

Anlotinib synergistically improved the anti-tumor efficacy of anti-PD-L1 *in vivo.* This study investigated the effects of Anlotinib on the anti-tumor efficacy of PD-L1 blockade. As presented in Figures 5A and 5B, lower xenograft tumor volume and weight were displayed in the Anlotinib group and the Anti-PD-L1 group when compared with the NC group (p<0.01). Interestingly, compared with the Anlotinib group and the Anti-PD-L1 group, the xenograft tumor volume and weight were both decreased in the Anlotinib+Anti-PD-L1 group (p<0.01). CD3+ and CD8+ T cells are two subpopulations of T cells, which exert an anti-tumor immune response by repressing the immune escape of tumor cells [19, 20]. Therefore, the expression of CD3+ and CD8+ T cells in xenograft tumors was explored by IHC. Relative to the NC group, Anlotinib or anti-PD-L1 promoted the number of CD3+ and CD8+ T cells in tumor tissue. The combination treatment of Anlotinib and anti-PD-L1 showed a synergistic reaction (Figure 5C). The expression of cytotoxic effector cytokines was detected by qRT-PCR. As shown in
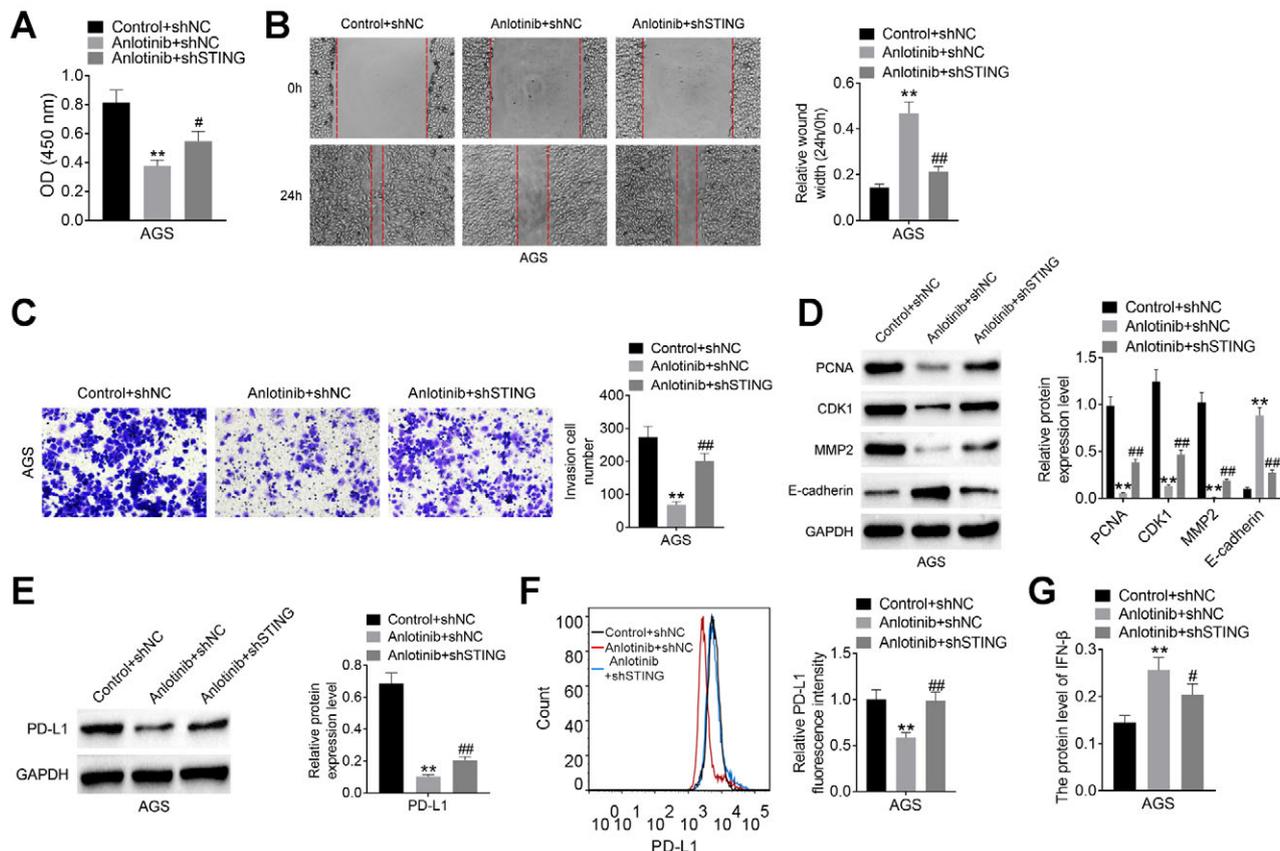
Figure 3. Anlotinib knockdown promoted gastric cancer cells' proliferation, migration, and immune escape by reducing the cGAS-STING/IFN-β pathway activity. A) Proliferation of gastric cancer cells by CCK-8 assay. **p<0.01 vs. the Control+shNC group; #p<0.05 vs. the Anlotinib+shNC group. **B)** Migration of gastric cancer cells by wound-healing experiment. **p<0.01 vs. the Control+shNC group; ##p<0.01 vs. the Anlotinib+shNC group. **C)** Invasion of gastric cancer cells by Transwell experiment. **p<0.01 vs. the Control+shNC group; ##p<0.01 vs. the Anlotinib+shNC group. **D)** Protein expressions in gastric cancer cells by eestern blot. **p<0.01 vs. the Control+shNC group; ##p<0.01 vs. the Anlotinib+shNC group. **E)** PD-L1 protein expression by western blot. **p<0.01 vs. the Control+shNC group and the Anlotinib+shSTING group. **F)** PD-L1 fluorescence intensity in gastric cancer cells by flow cytometry. **p<0.01 vs. the Control+shNC group and the Anlotinib+shSTING group. **G)** IFN-β level in gastric cancer cells by ELISA. **p<0.01 vs. the Control+shNC group; #p<0.05 vs. the Anlotinib+shNC group.

Figures 5D–F, compared with the NC group, Anlotinib or anti-PD-L1 treatment increased the expression of cytotoxic effector cytokines (granzyme B, TNF-α, and IFN-g), tumor-suppressive chemokines (CCL5, CXCL9, and CXCL10) and immunosurveillance enhancing interleukins (IL1b, IL12b, and IL15), whereas inhibited tumor-promoting cytokines (IL17a) expression (p<0.05 or p<0.01). In comparison with the Anlotinib group or the Anti-PD-L1 group, the combination treatment of Anlotinib and anti-PD-L1 showed a synergistic reaction in regulating the expression of these above cytotoxic effector cytokines (p<0.05 or p<0.01).
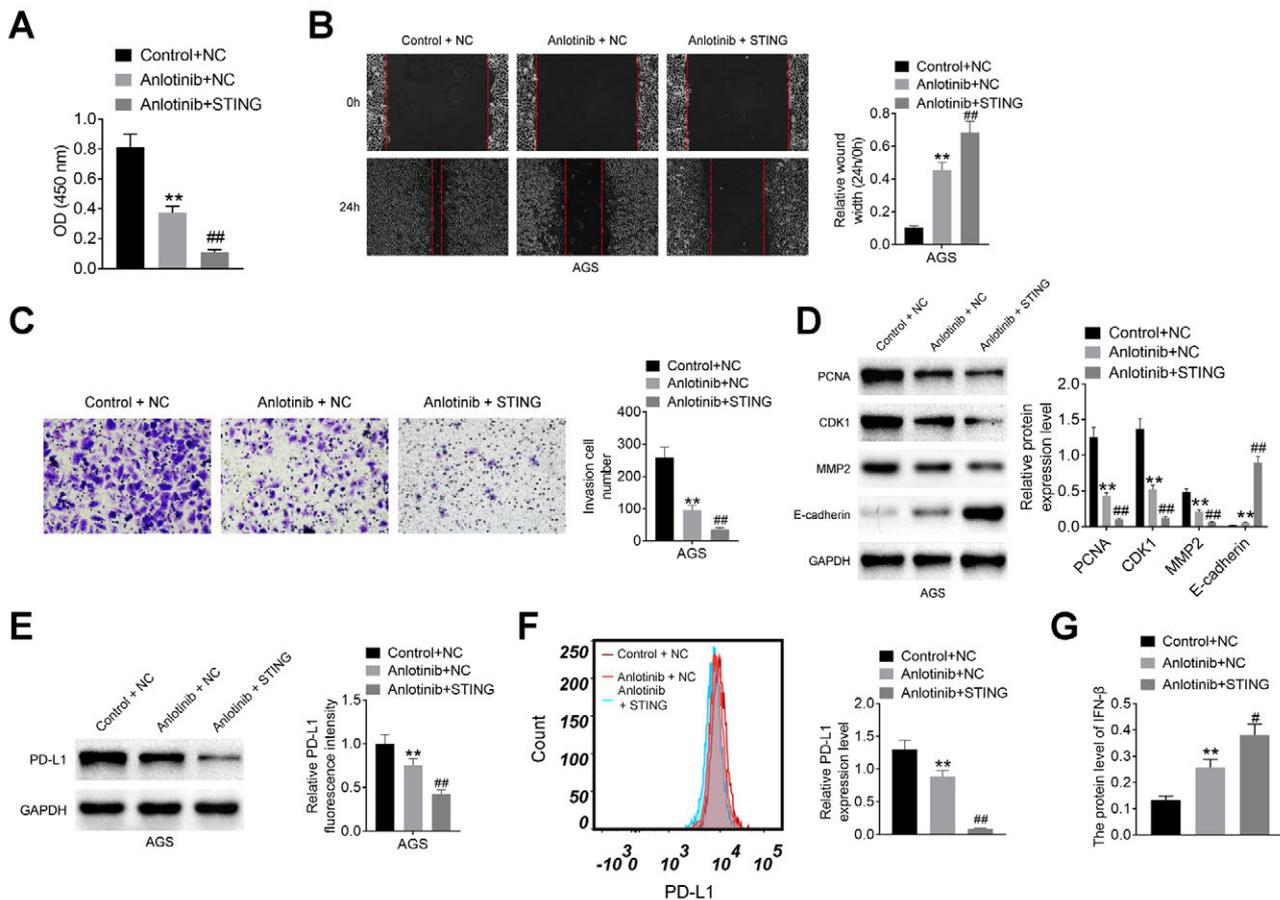
Anlotinib activated the cGAS-STING/IFN-β pathway in xenograft tumors and was non-toxic to lung, liver, cortex, and kidneys. The cGAS, STING, and IFN-β expression in xenograft tumors was reflected by IHC. As exhibited in Figure 6, xenograft tumors of the Anlotinib group and the Anti-PD-L1 group presented more cGAS, STING, and IFN-β positive particles than that of the NC group. Simul-

taneously, more cGAS, STING, and IFN-β positive particles were observed in xenograft tumors of the Anlotinib+Anti-PD-L1 group when compared with the Anlotinib group and the Anti-PD-L1 group.

The damage of Anlotinib to other organs of mice, including lung, liver, cortex, and kidneys, was detected by HE staining. The results are shown in Figure 6B. It could be seen that the lung, liver, cortex, and kidney tissue of mice in the four groups were arranged tightly and regularly. Cells had a regular structure. These phenomena indicated that Anlotinib was non-toxic to lung, liver, cortex, and kidneys of mice.

Discussion

In this study, Anlotinib at a dose of 8 μM could effectively suppress gastric cancer cells' proliferation, migration, and invasion *in vitro*. Proliferating cell nuclear antigen (PCNA) possesses the ability to enhance tumor cell proliferation

Figure 4. Anlotinib inhibited gastric cancer cells' proliferation, migration, and immune escape by activating the cGAS-STING/IFN-β pathway. A) Proliferation of gastric cancer cells by CCK-8 assay. B) Migration of gastric cancer cells by wound-healing experiment. C) Invasion of gastric cancer cells by Transwell experiment. D) Protein expressions in gastric cancer cells by western blot. E) PD-L1 protein expression by western blot. F) PD-L1 fluorescence intensity in gastric cancer cells by flow cytometry. G) IFN-β level in gastric cancer cells by ELISA. **p<0.01 vs. the Control+NC group; #p<0.05 and ##p<0.01 vs. the Anlotinib+NC group

through participating in DNA metabolism (such as DNA replication and repair, etc.) and energy metabolism (such as glycolysis) [21, 22]. Cyclin-dependent kinase 1 (CDK1) is a member of the CDK family, which is essential for driving cell cycle progression [23]. CDK1 upregulation promotes tumor cell proliferation via accelerating cell cycle progression and is associated with multiple tumors progression [24]. In this study, it was detected that Anlotinib at a dose of 8 μM decreased the expression of PCNA and CDK1 proteins in gastric cancer cells. Thus, Anlotinib might suppress gastric cancer cells' proliferation by reducing PCNA and CDK1 protein expressions. Additionally, matrix metalloproteinase 2 (MMP-2) and E-cadherin are two well-known genes related to epithelial-to-mesenchymal transition (EMT). MMP-2 is a Zn^{2+} dependent endopeptidase, which is famous for promoting tumor invasion and metastasis via degrading type IV collagen [25]. MMP-2 high expression has been identified to facilitate unfavorable prognosis in multiple malignant tumors [26, 27]. The downregulation of E-cadherin is

considered to be a key event during EMT. E-cadherin could enhance cell-cell adhesion, and then prevent the separation of individual cells from the primary tumor mass. E-cadherin downregulation often indicated metastasis of tumors [28]. Anlotinib at a dose of 8 μM was observed to reduce MMP-2 expression and elevate E-cadherin expression in gastric cancer cells. This indicated that Anlotinib might inhibit gastric cancer cells' migration and invasion by decreasing MMP-2 expression and increasing E-cadherin expression.

This study researched the effect of Anlotinib on immune escape in gastric cancer cells. Data illustrated that Anlotinib reduced the expression of PD-L1 in gastric cancer cells. The highly expressed PD-L1 in tumor cells usually binds to programmed cell death receptor 1 (PD-1) on activated T cells. This process causes a decreased activity or increased apoptosis of T cells and eventually leads to immune escape [29, 30]. Therefore, interaction blockade between PD-L1 and PD-1 can augment the T-cell response to enhance antitumor activity [31]. A previous study had discovered that
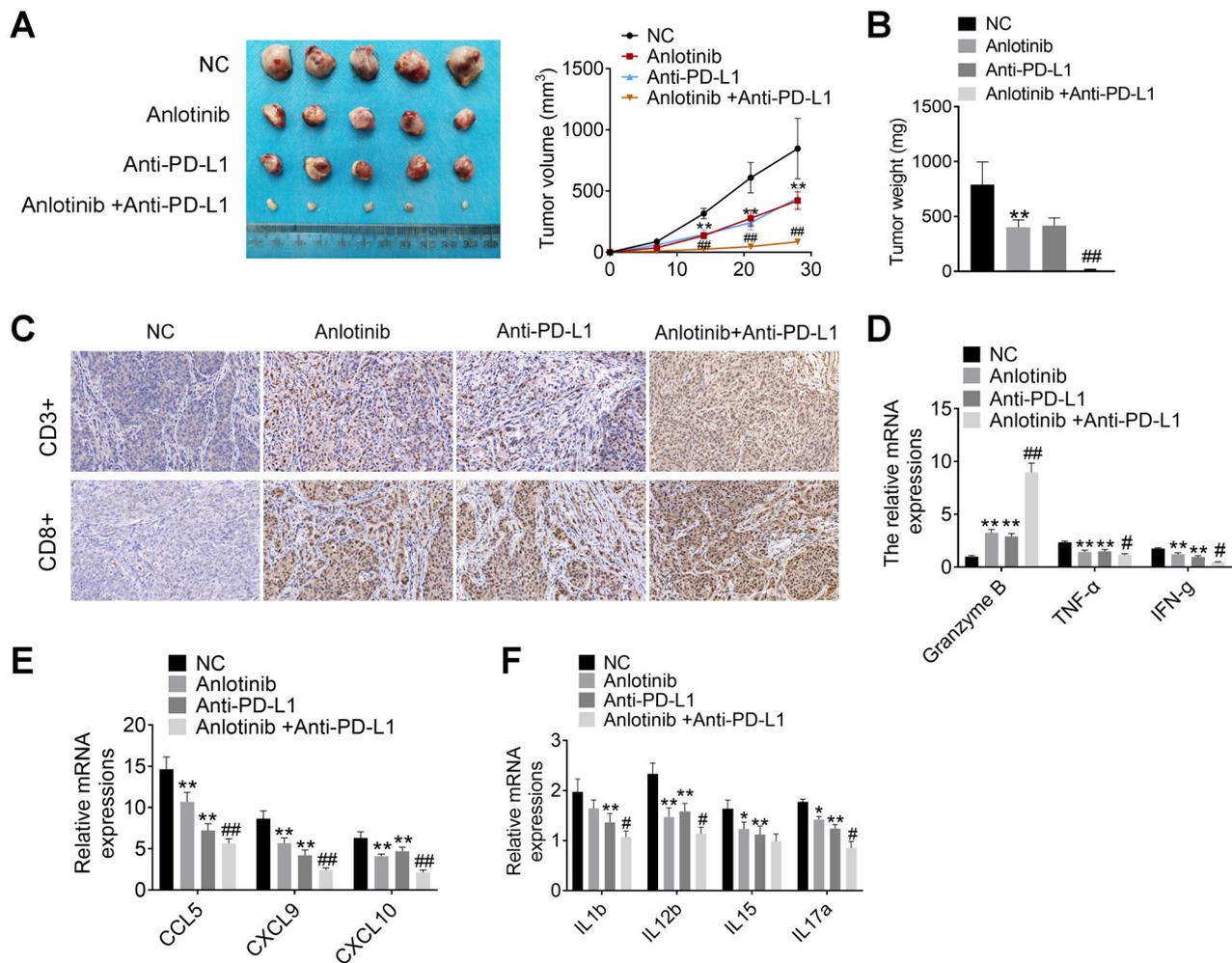
Figure 5. Anlotinib synergistically improved the anti-tumor efficacy of anti-PD-L1 *in vivo*. A) Photographs of xenograft tumor and xenograft tumor volume curves. B) Xenograft tumor weight in nude mice. C) The expression of CD3+ and CD8+ T cells in tumor tissue was explored by IHC. D–F) The expression of cytotoxic effector cytokines was detected by qRT-PCR. *p<0.05 and **p<0.01 vs. the NC group. #p<0.05 and ##p<0.01 vs. the Anlotinib group and the Anti-PD-L1 group

the upregulated PD-L1 facilitated the resistance of gastric cancer cells to the immune responses. PD-L1 high expression helped gastric cancer cells escape T cells killing, and then enhanced gastric cancer cells' proliferation [32, 33]. This study revealed that Anlotinib could suppress gastric cancer cells' immune escape by reducing PD-L1 expression. *In vivo* data indicated that Anlotinib reduced gastric cancer cells' growth in mice. The clinical application had demonstrated that the anti-PD-L1 antibody had well safety and activity in multiple types of advanced cancer patients. The anti-PD-L1 antibody prolonged tumor stabilization and induced durable tumor regression [34]. In advanced gastric cancer, the anti-PD-L1 antibody therapy exhibited effective and safe anti-tumor activity and tolerable adverse effects [35, 36]. This study exhibited that the anti-PD-L1 antibody treatment suppressed gastric cancer cell growth in mice. More interest-

ingly, Anlotinib and anti-PD-L1 synergistically suppressed gastric cancer cells' growth in mice. Thus, Anlotinib might be an effective drug for gastric cancer treatment.

More importantly, this research explored that Anlotinib increased the expression of cGAS, STING, and IFN-β in gastric cancer cells and xenograft tumors. STING knockdown partially reversed the inhibitory effect of Anlotinib on gastric cancer cells proliferation, migration, invasion, and immune escape. However, STING overexpression enhanced the inhibition of Anlotinib on the above malignant phenotype of gastric cancer cells. According to these data, it was inferred that Anlotinib might suppress gastric cancer malignant phenotype and immune escape by reducing PD-L1 expression via activating the cGAS-STING/IFN-β pathway. A previous study revealed that the activated cGAS-STING pathway possessed an anti-tumorigenic role
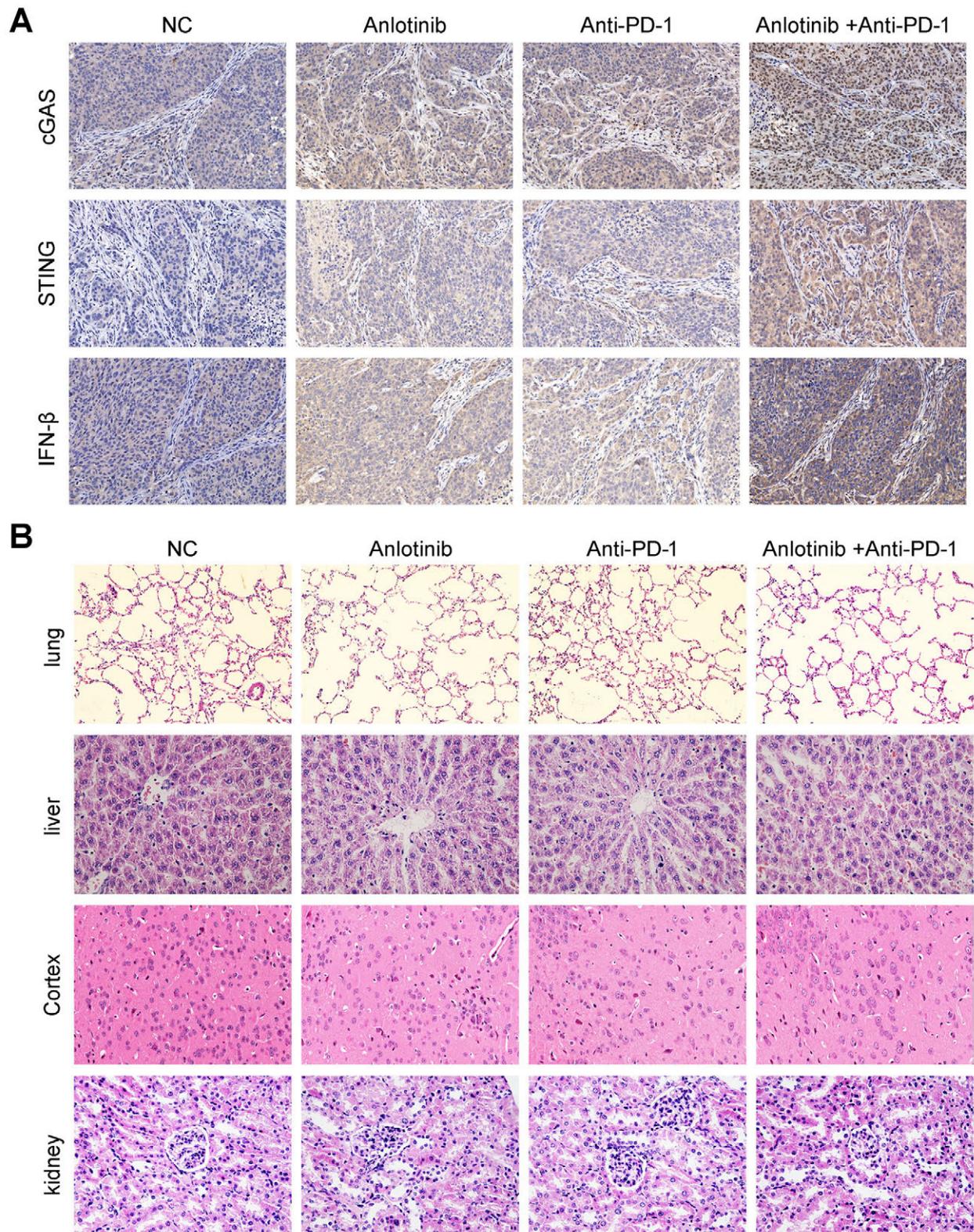
Figure 6. Anlotinib activated the cGAS-STING/IFN-β pathway in xenograft tumors and was non-toxic to lung, liver, cortex, and kidneys. A) The expression of cGAS, STING, and IFN-β proteins in xenograft tumors was detected by IHC. B) HE staining was applied for the damage detection of Anlotinib to other organs, including lung, liver, cortex, and kidneys.

by activating T cells for tumor control [37]. cGAS-STING agonist had been proposed to be used as a sensitizer for several tumor immunotherapies [38]. Recent data revealed that the efficacy of multiple anti-tumor therapies depended on the cGAS-STING pathway activation, especially clinical immunotherapy [39]. IFN-β was originally identified as one of the immunomodulatory cytokines because of its antiviral activity [40]. As a downstream signal of cGAS-STING, IFN-β expression was discovered to be STING-dependent [37]. Recent data indicated that IFN-β had strong anti-tumor effects, such as anti-proliferation, apoptosis induction, immunomodulatory activities, arresting of the cell cycle, and chemotherapy sensitivity enhancement. IFN-β was thus suggested to be used for malignant tumor treatment and immune-mediated diseases [40–42]. This study demonstrated for the first time that Anlotinib might exhibit its anti-tumor effect in gastric cancer by activating the cGAS-STING/IFN-β pathway.

CD3+ T cells, the main subpopulation of T cells, can suppress tumor cells' immune escape [19]. The toxicity of CD3+ T cells to tumor cells makes it a promising immunotherapy strategy for the treatment of solid tumors [43]. As another subpopulation of T cells, CD8+ T cells can mediate the anti-tumor immune response, which can infiltrate the tumor site to kill tumor cells [20]. In this study, Anlotinib synergistic anti-PD-L1 increased CD3+ and CD8+ T cells in xenograft tumors. This research also revealed that Anlotinib synergistic anti-PD-L1 increased the expression of cytotoxic effector cytokines (granzyme B, TNF-α, IFN-g), tumor-suppressive chemokines (CCL5, CXCL9, CXCL10), immunosurveillance enhancing interleukins (IL1b, IL12b, IL15), whereas inhibited tumor-promoting cytokines (IL17a) expression. This discovery provided more reliable evidence for the use of Anlotinib in gastric cancer treatment. Additionally, by HE staining, the toxicity of Anlotinib to other vital organs was investigated. The results indicated that Anlotinib was non-toxic to lung, liver, cortex, and kidneys of mice. Thus, Anlotinib was effective and safe in the treatment of gastric cancer.

There is a limitation in this study. It may be more convincing if more data were provided on other molecules on the IFN-β pathway. However, these studies cannot currently be performed due to laboratory limitations. This will be the focus of our future research. This paper researched the effect of Anlotinib in gastric cancer treatment. The results illustrated that Anlotinib effectively suppressed gastric cancer cells' proliferation, migration, and immune escape by activating the cGAS-STING/IFN-β pathway. *In vivo* data indicated that Anlotinib obviously inhibited gastric cancer cell growth and activated the cGAS-STING/IFN-β pathway. Moreover, Anlotinib might be safe in gastric cancer treatment, as it was non-toxic to lung, liver, cortex, and kidneys of mice. All of the results suggested that Anlotinib was effective and safe in the treatment of gastric cancer. It could be applied in gastric cancer treatment clinically.

References

[1] WU T, WU L. The role and clinical implications of the retinoblastoma (RB)-E2F pathway in gastric cancer. Front Oncol 2021; 11: 655630. https://doi.org/10.3389/fonc.2021.655630

[2] LUTZ MP, ZALCBERG JR, DUCREUX M, ADENIS A, ALLUM W et al. The 4th St. Gallen EORTC Gastrointestinal Cancer Conference: Controversial issues in the multimodal primary treatment of gastric, junctional and oesophageal adenocarcinoma. Eur J Cancer 2019; 112: 1–8. https://doi.org/10.1016/j.ejca.2019.01.106

[3] MA Y, ZHOU A, SONG J. Upregulation of miR-1307-3p and its function in the clinical prognosis and progression of gastric cancer. Oncol Lett 2021; 21: 91. https://doi.org/10.3892/ol.2020.12352

[4] HAN X, LIU Z. Long non-coding RNA JPX promotes gastric cancer progression by regulating CXCR6 and autophagy via inhibiting miR-197. Mol Med Rep, 2021; 23: 60. https://doi.org/10.3892/mmr.2020.11698

[5] TANG J, HU Y, ZHANG C, GONG C. miR-4636 inhibits tumor cell proliferation, migration and invasion, and serves as a candidate clinical biomarker for gastric cancer. Oncol Lett 2021; 21: 33. https://doi.org/10.3892/ol.2020.12294

[6] COHEN R, PUDLARZ T, GARCIA-LARNICOL ML, VERNEREY D, DRAY X et al. Localized MSI/dMMR gastric cancer patients, perioperative immunotherapy instead of chemotherapy: The GERCOR NEONIPIGA phase II study is opened to recruitment. Bull Cancer 2020; 107: 438–446. https://doi.org/10.1016/j.bulcan.2019.11.016

[7] KOSAKA T, AKIYAMA H, MIYAMOTO H, SATO S, TANAKA Y et al. Outcomes of preoperative S-1 and docetaxel combination chemotherapy in patients with locally advanced gastric cancer. Cancer Chemother Pharmacol 2019; 83: 1047–1055. https://doi.org/10.1007/s00280-019-03813-6

[8] SUN Y, NIU W, DU F, DU C, Li S et al. Safety, pharmacokinetics, and antitumor properties of anlotinib, an oral multitarget tyrosine kinase inhibitor, in patients with advanced refractory solid tumors. J Hematol Oncol 2016; 9: 105. https://doi.org/10.1186/s13045-016-0332-8

[9] HAN B, LI K, WANG Q, ZHANG L, SHI J et al. Effect of Anlotinib as a Third-Line or Further Treatment on Overall Survival of Patients With Advanced Non-Small Cell Lung Cancer: The ALTER 0303 Phase 3 Randomized Clinical Trial. JAMA Oncol 2018; 4: 1569–1575. https://doi.org/10.1001/jamaoncol.2018.3039

[10] WANG Y, LIANG D, CHEN J, CHEN H, FAN R et al. Targeted Therapy with Anlotinib for a Patient with an Oncogenic FGFR3-TACC3 Fusion and Recurrent Glioblastoma. Oncologist 2021; 26: 173–177. https://doi.org/10.1002/onco.13530

[11] CHI Y, SHU Y, BA Y, BAI Y, QIN B et al. Anlotinib Monotherapy for Refractory Metastatic Colorectal Cancer: A Double-Blinded, Placebo-Controlled, Randomized Phase III Trial (ALTER0703). Oncologist 2021; 26: e1693–e1703. https://doi.org/10.1002/onco.13857

[12] ZHONG Y, WEI Q, LU Y, TANG X, WANG Z et al. Efficacy and safety of anlotinib in patients with advanced non-small cell lung cancer. J Thorac Dis 2020; 12: 6016–6022. https://doi.org/10.21037/jtd-20-2855

[13] CUI Q, HU Y, MA D, LIU H. A Retrospective Observational Study of Anlotinib in Patients with Platinum-Resistant or Platinum-Refractory Epithelial Ovarian Cancer. Drug Des Devel Ther 2021; 15: 339–347. https://doi.org/10.2147/DDDT.S286529

[14] LUO Q, ZHANG S, ZHANG D, FENG R, LI N et al. Effects and Mechanisms of Anlotinib and Dihydroartemisinin Combination Therapy in Ameliorating Malignant Biological Behavior of Gastric Cancer Cells. Curr Pharm Biotechnol 2021; 22: 523–533. https://doi.org/10.2174/1389201021666200623132803

[15] WANG J, WU DX, MENG L, JI G. Anlotinib combined with SOX regimen (S1 (tegafur, gimeracil and oteracil porassium capsules) + oxaliplatin) in treating stage IV gastric cancer: study protocol for a single-armed and single-centred clinical trial. BMJ Open 2020; 10: e034685. https://doi.org/10.1136/bmjopen-2019-034685

[16] JIANG X, WANG J, DENG X, XIONG F, GE J et al. Role of the tumor microenvironment in PD-L1/PD-1-mediated tumor immune escape. Mol Cancer 2019; 18: 10. https://doi.org/10.1186/s12943-018-0928-4

[17] ZHU D, XU R, HUANG X, TABG Z, TIAN Y et al. Deubiquitinating enzyme OTUB1 promotes cancer cell immunosuppression via preventing ER-associated degradation of immune checkpoint protein PD-L1. Cell Death Differ 2021; 28: 1773–1789. https://doi.org/10.1038/s41418-020-00700-z

[18] YANG Y, LI L, JIANG Z, WANG B, PAN Z. Anlotinib optimizes anti-tumor innate immunity to potentiate the therapeutic effect of PD-1 blockade in lung cancer. Cancer Immunol Immunother 2020; 69: 2523–2532. https://doi.org/10.1007/s00262-020-02641-5

[19] CHEN N, FANG W, LIN Z, PENG P, WANG J et al. KRAS mutation-induced upregulation of PD-L1 mediates immune escape in human lung adenocarcinoma. Cancer Immunol Immunother 2017; 66: 1175–1187. https://doi.org/10.1007/s00262-017-2005-z

[20] FARHOOD B, NAJAFI M, MORTEZAEE K. CD8+ cytotoxic T lymphocytes in cancer immunotherapy: A review. J Cell Physiol 2019; 234: 8509–8521. https://doi.org/10.1002/jcp.27782

[21] YE X, LING B, XU H, LI G, ZHAO X et al. Clinical significance of high expression of proliferating cell nuclear antigen in non-small cell lung cancer. Medicine (Baltimore) 2020; 99: e19755. https://doi.org/10.1097/MD.0000000000019755

[22] CARDANO M, TRIBIOLI C, PROSPERI E. Targeting Proliferating Cell Nuclear Antigen (PCNA) as an Effective Strategy to Inhibit Tumor Cell Proliferation. Curr Cancer Drug Targets 2020; 20: 240–252. https://doi.org/10.2174/1568009620666200115162814

[23] MALUMBRES M, BARBACID M. Cell cycle, CDKs and cancer: a changing paradigm. Nat Rev Cancer 2009; 9: 153–166. https://doi.org/10.1038/nrc2602

[24] ZHAO S, WANG B, MA Y, KUANG J, LIANG J et al. NUCKS1 Promotes Proliferation, Invasion and Migration of Non-Small Cell Lung Cancer by Upregulating CDK1 Expression. Cancer Manag Res 2020; 12: 13311–13323. https://doi.org/10.2147/CMAR.S282181

[25] LI S, LUO W. Matrix metalloproteinase 2 contributes to aggressive phenotype, epithelial-mesenchymal transition and poor outcome in nasopharyngeal carcinoma. Onco Targets Ther 2019; 12: 5701–5711. https://doi.org/10.2147/OTT.S202280

[26] ZHANG X, SHI G, GAO F, LIU P, WANG H et al. TSPAN1 upregulates MMP2 to promote pancreatic cancer cell migration and invasion via PLCγ. Oncol Rep 2019; 41: 2117–2125. https://doi.org/10.3892/or.2019.6989

[27] AKIZUKI R, EGUCHI H, ENDO S, MATSUNAGA T, IKARI A. ZO-2 Suppresses Cell Migration Mediated by a Reduction in Matrix Metalloproteinase 2 in Claudin-18-Expressing Lung Adenocarcinoma A549 Cells. Biol Pharm Bull 2019; 42: 247–254. https://doi.org/10.1248/bpb.b18-00670

[28] SOMMARIVA M, GAGLIANO N. E-Cadherin in Pancreatic Ductal Adenocarcinoma: A Multifaceted Actor during EMT. Cells 2020; 9: 1040. https://doi.org/10.3390/cells9041040

[29] LIU C, YAO Z, WABG J, ZHANG W, YANG Y et al. Macrophage-derived CCL5 facilitates immune escape of colorectal cancer cells via the p65/STAT3-CSN5-PD-L1 pathway. Cell Death Differ 2020; 27: 1765–1781. https://doi.org/10.1038/s41418-019-0460-0

[30] XIE F, XU M, LU J, MAO L, WANG S. The role of exosomal PD-L1 in tumor progression and immunotherapy. Mol Cancer 2019; 18: 146. https://doi.org/10.1186/s12943-019-1074-3

[31] DERMANI FK, SAMADI P, RAHMANI G, KOHLAN AK, NAJAFI R. PD-1/PD-L1 immune checkpoint: Potential target for cancer therapy. J Cell Physiol 2019; 234: 1313–1325. https://doi.org/10.1002/jcp.27172

[32] DANG S, MALIK A, CHEN J, QU J, YIN K et al. LncRNA SNHG15 Contributes to Immuno-Escape of Gastric Cancer Through Targeting miR141/PD-L1. Onco Targets Ther 2020; 13: 8547–8556. https://doi.org/10.2147/OTT.S251625

[33] JU X, ZHANG H, ZHOU Z, CHEN M, WANG Q. Tumor-associated macrophages induce PD-L1 expression in gastric cancer cells through IL-6 and TNF-α signaling. Exp Cell Res 2020; 396: 112315. https://doi.org/10.1016/j.yexcr.2020.112315

[34] BRAHMER JR, TYKODI SS, CHOW LQ, HWU WJ, TOPALIAN SL et al. Safety and activity of anti-PD-L1 antibody in patients with advanced cancer. N Engl J Med 2012; 366: 2455–2465. https://doi.org/10.1056/NEJMoa1200694

[35] NI X, XING Y, SUN X, SUO J. The safety and efficacy of anti-PD-1/anti-PD-L1 antibody therapy in the treatment of previously treated, advanced gastric or gastro-oesophageal junction cancer: A meta-analysis of prospective clinical trials. Clin Res Hepatol Gastroenterol 2020; 44: 211–222. https://doi.org/10.1016/j.clinre.2019.05.007

[36] YANG L, DONG XZ, XING XX, CUI XH, LI L et al. Efficacy and safety of anti-PD-1/anti-PD-L1 antibody therapy in treatment of advanced gastric cancer or gastroesophageal junction cancer: A meta-analysis. World J Gastrointest Oncol 2020; 12: 1346–1363. https://doi.org/10.4251/wjgo.v12.i11.1346

[37]   KHOO LT, CHEN LY. Role of the cGAS-STING pathway in cancer development and oncotherapeutic approaches. EMBO Rep 2018; 19: e46935. https://doi.org/10.15252/embr.201846935

[38]   LI A, YI M, QIN S, SONG Y, CHU Q et al. Activating cGAS-STING pathway for the optimal effect of cancer immunotherapy. J Hematol Oncol 2019; 12: 35. https://doi.org/10.1186/s13045-019-0721-x

[39]   LV M, CHEN M, ZHANG R, ZHANG W, WANG C et al. Manganese is critical for antitumor immune responses via cGAS-STING and improves the efficacy of clinical immunotherapy. Cell Res 2020; 30: 966–979. https://doi.org/10.1038/s41422-020-00395-4

[40]   BLAAUBOER A, BOOY S, VAN KOETSVELD PM, KARELS B, DOGAN F et al. Interferon-beta enhances sensitivity to gemcitabine in pancreatic cancer. BMC Cancer 2020; 20: 913. https://doi.org/10.1186/s12885-020-07420-0

[41]   KLOTZ D, BAUMGARTNER W, GERHAUSER I. Type I interferons in the pathogenesis and treatment of canine diseases. Vet Immunol Immunopathol 2017; 191: 80–93. https://doi.org/10.1016/j.vetimm.2017.08.006

[42]   SIMS TL, MCGEE M, WILLIAMS RF, MYERS AL, TRACEY L et al. IFN-beta restricts tumor growth and sensitizes alveolar rhabdomyosarcoma to ionizing radiation. Mol Cancer Ther 2010; 9: 761–771. https://doi.org/10.1158/1535-7163.MCT-09-0800

[43]   SINGH A, DEES S, GREWAL IS. Overcoming the challenges associated with CD3+ T-cell redirection in cancer. Br J Cancer 2021; 124: 1037–1048. https://doi.org/10.1038/s41416-020-01225-5